Cell Reports, Volume *42*

Supplemental information

KEAP1 mutation in lung adenocarcinoma promotes immune evasion and immunotherapy resistance

Anastasia-Maria Zavitsanou, Ray Pillai, Yuan Hao, Warren L. Wu, Eric Bartnicki, Triantafyllia Karakousi, Sahith Rajalingam, Alberto Herrera, Angeliki Karatza, Ali Rashidfarrokhi, Sabrina Solis, Metamia Ciampricotti, Anna H. Yeaton, Ellie Ivanova, Corrin A. Wohlhieter, Terkild B. Buus, Makiko Hayashi, Burcu Karadal-Ferrena, Harvey I. Pass, John T. Poirier, Charles M. Rudin, Kwok-Kin Wong, Andre L. Moreira, Kamal M. Khanna, Aristotelis Tsirigos, Thales Papagiannakopoulos, and Sergei B. Koralov

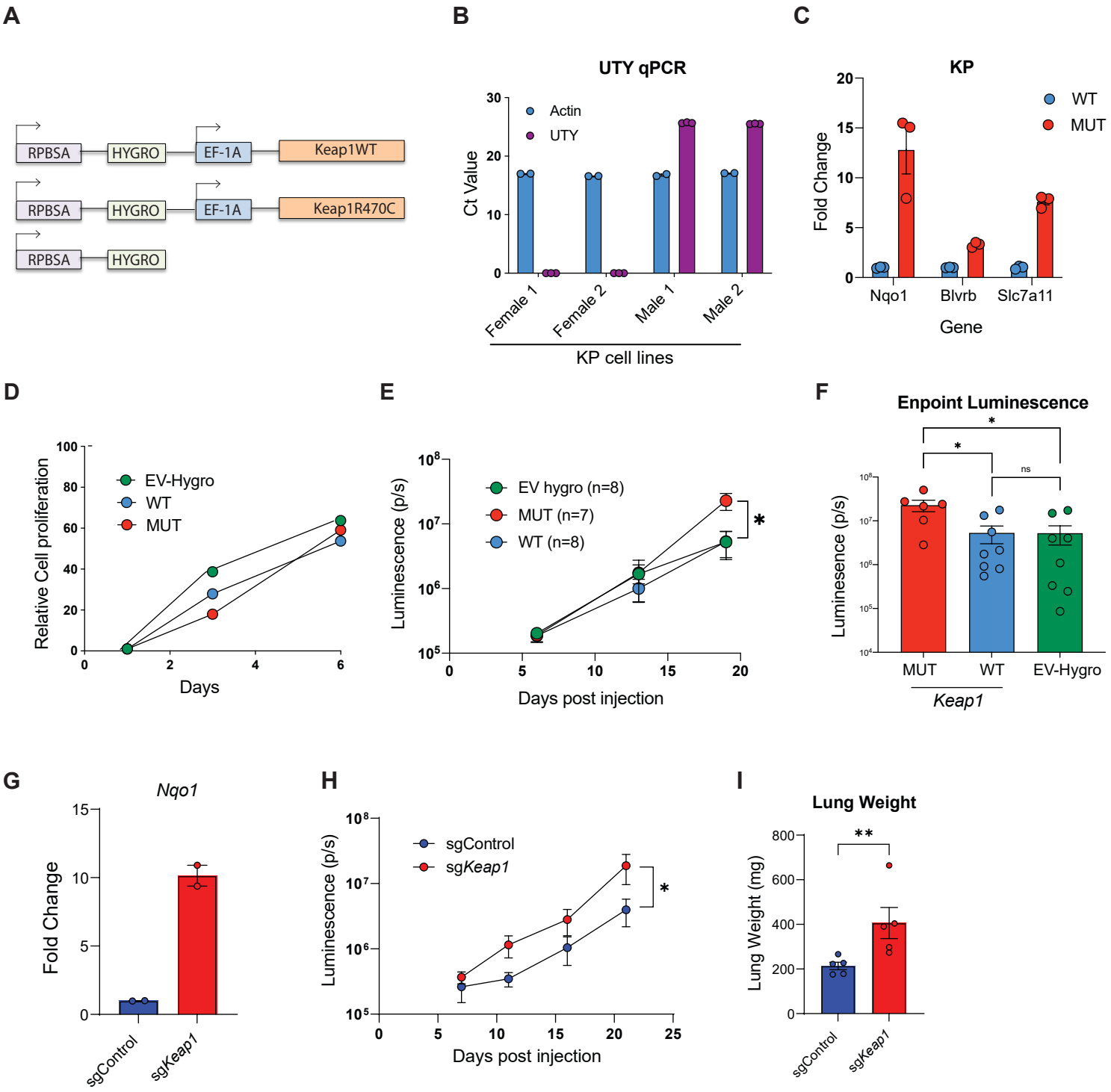
A
RPBSA
HYGRO
EF-1A
Keap1WT
RPBSA
HYGRO
EF-1A
Keap1R470C
RPBSA
HYGRO
B
UTY qPCR
Actin
UTY
Ct Value
Female 1
Female 2
Male 1
Male 2
KP cell lines
C
KP
WT
MUT
Fold Change
Nqo1
Blvrb
Slc7a11
Gene
D
EV-Hygro
WT
MUT
Relative Cell proliferation
Days
E
EV hygro (n=8)
MUT (n=7)
WT (n=8)
Luminescence (p/s)
Days post injection
F
Enpoint Luminescence
ns
Luminescence (p/s)
MUT
WT
EV-Hygro
Keap1
G
Nqo1
Fold Change
sgControl
sgKeap1
H
sgControl
sgKeap1
Luminescence (p/s)
Days post injection
I
Lung Weight
Lung Weight (mg)
sgControl
sgKeap1

Fig. S1

Supplementary Fig 1: Impact of *Keap1* genetic inactivation on tumor growth in mouse models of LUAD.

(A) Schematic of vectors overexpressing wild-type or mutant *Keap1* and empty vector control used to modify cell lines in the orthotopic LUAD model. (B) Gene expression of *Uty* in KP cell lines isolated from female or male animals. KP cell line male 2 was selected for subsequent experiments (C) Gene expression of Nrf2 target genes in KP cells overexpressing wild-type (WT) or mutant (MUT) *Keap1*. (D) *In vitro* proliferation analysis of KP cell lines transduced with vectors shown in A reveals no difference in growth kinetics. (EV: empty vector) (E) Growth kinetics analysis of KP cells expressing *Keap1* wild-type, mutant or empty vector control in C57BL/6J female hosts as measured by bioluminescence reveals increased proliferation by *Keap1*-mutant cells (F) Endpoint luminescence of a representative experiment outlined in E. (G) QPCR showing *Nqo1* expression of *Keap1* knockout (sg*Keap1*) cell lines *in vitro* relative to controls. (H) Growth of sg*Keap1* KP cells and controls *in vivo* after IV injection into female C57BL/6J mice as measured by bioluminescence. (I) Weight of tumor bearing lungs from mice in H on day 21. *P<0.05; **P<0.01

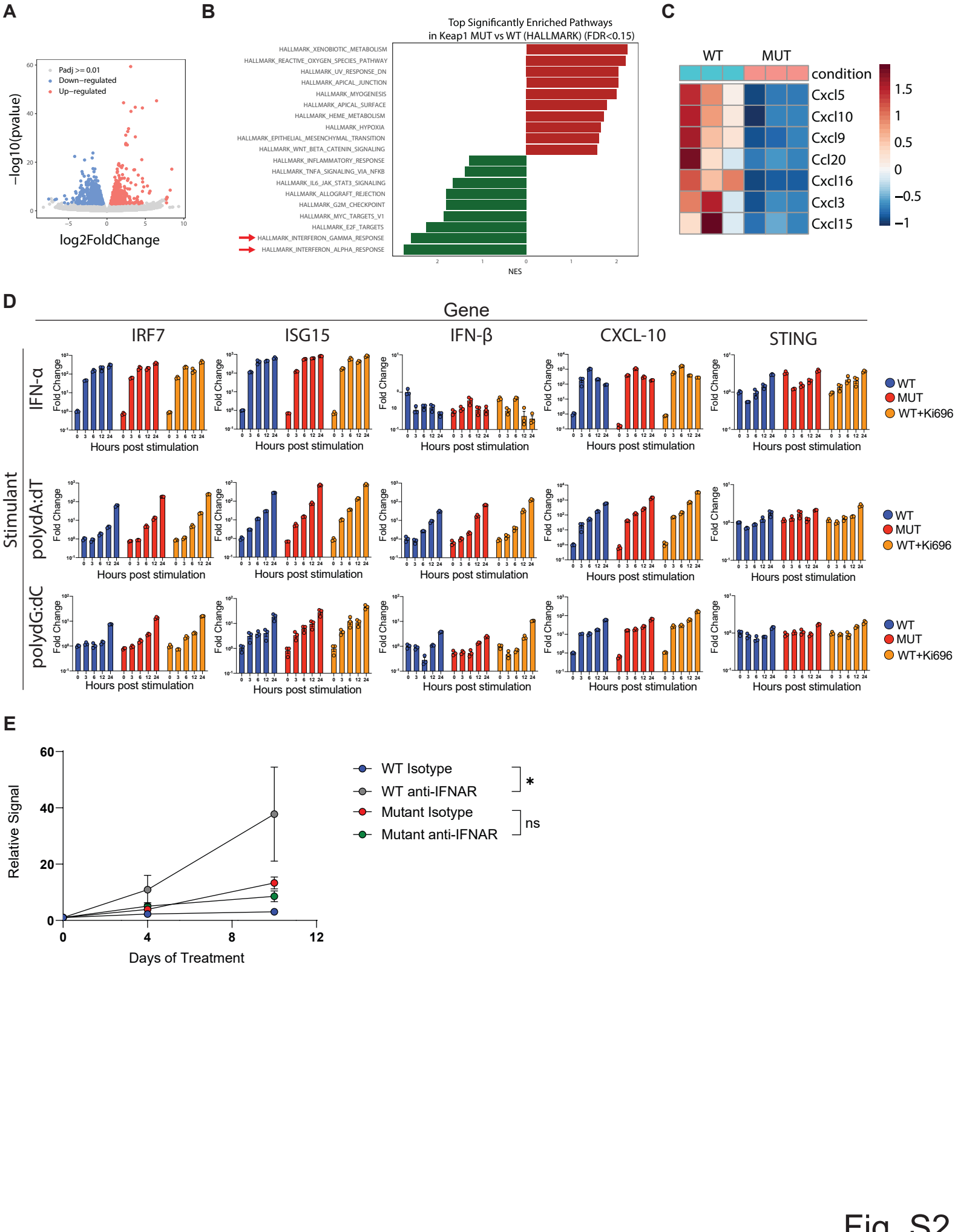
A
Padj >= 0.01
Down−regulated
Up−regulated
−log10(pvalue)
log2FoldChange
B
Top Significantly Enriched Pathways
in Keap1 MUT vs WT (HALLMARK) (FDR<0.15)
HALLMARK_XENOBIOTIC_METABOLISM
HALLMARK_REACTIVE_OXYGEN_SPECIES_PATHWAY
HALLMARK_UV_RESPONSE_DN
HALLMARK_APICAL_JUNCTION
HALLMARK_MYOGENESIS
HALLMARK_APICAL_SURFACE
HALLMARK_HEME_METABOLISM
HALLMARK_HYPOXIA
HALLMARK_EPITHELIAL_MESENCHYMAL_TRANSITION
HALLMARK_WNT_BETA_CATENIN_SIGNALING
HALLMARK_INFLAMMATORY_RESPONSE
HALLMARK_TNFA_SIGNALING_VIA_NFKB
HALLMARK_IL6_JAK_STAT3_SIGNALING
HALLMARK_ALLOGRAFT_REJECTION
HALLMARK_G2M_CHECKPOINT
HALLMARK_MYC_TARGETS_V1
HALLMARK_E2F_TARGETS
HALLMARK_INTERFERON_GAMMA_RESPONSE
HALLMARK_INTERFERON_ALPHA_RESPONSE
NES
C
WT
MUT
condition
Cxcl5
Cxcl10
Cxcl9
Ccl20
Cxcl16
Cxcl3
Cxcl15
1.5
1
0.5
0
−0.5
−1
D
Gene
IRF7
ISG15
IFN-β
CXCL-10
STING
Stimulant
IFN-α
polydA:dT
polydG:dC
Fold Change
Hours post stimulation
WT
MUT
WT+Ki696
E
Relative Signal
Days of Treatment
WT Isotype
WT anti-IFNAR
Mutant Isotype
Mutant anti-IFNAR
*
ns

Fig. S2

Supplementary Fig 2: *Keap1*-mutant tumors have reduced interferon signaling *in vivo.*

(A) RNA-seq was performed on sorted *Keap1*-mutant and wildtype tumors. Volcano plot showing differentially expressed genes in mutant tumors vs wildtype tumors. (B) Most significantly enriched or depleted pathways (FDR <0.15) in *Keap1*-mutant (MUT) compared to wild-type (WT) tumor cells isolated via sorting from tumor-bearing female hosts and subjected to RNA-seq. (C) Gene expression heatmap of chemokines significantly ($p<0.05$) altered between *Keap1*-mutant and wild-type tumors. (D) *Keap1*-mutant, *Keap1*-wildtype, or *Keap1*-wildtype + Ki696 treated tumor cells were stimulated with either IFN-α, polydA:dT, or polyG:dC *in vitro*. QPCR was performed looking at relative expression of specified gene targets at the indicated timepoints. (E) Growth kinetics of *Keap1*-mutant and wildtype tumors as measured by bioluminescence in C57BL/6J female mice after treatment with either anti-IFNAR antibody or isotype control. *P<0.05

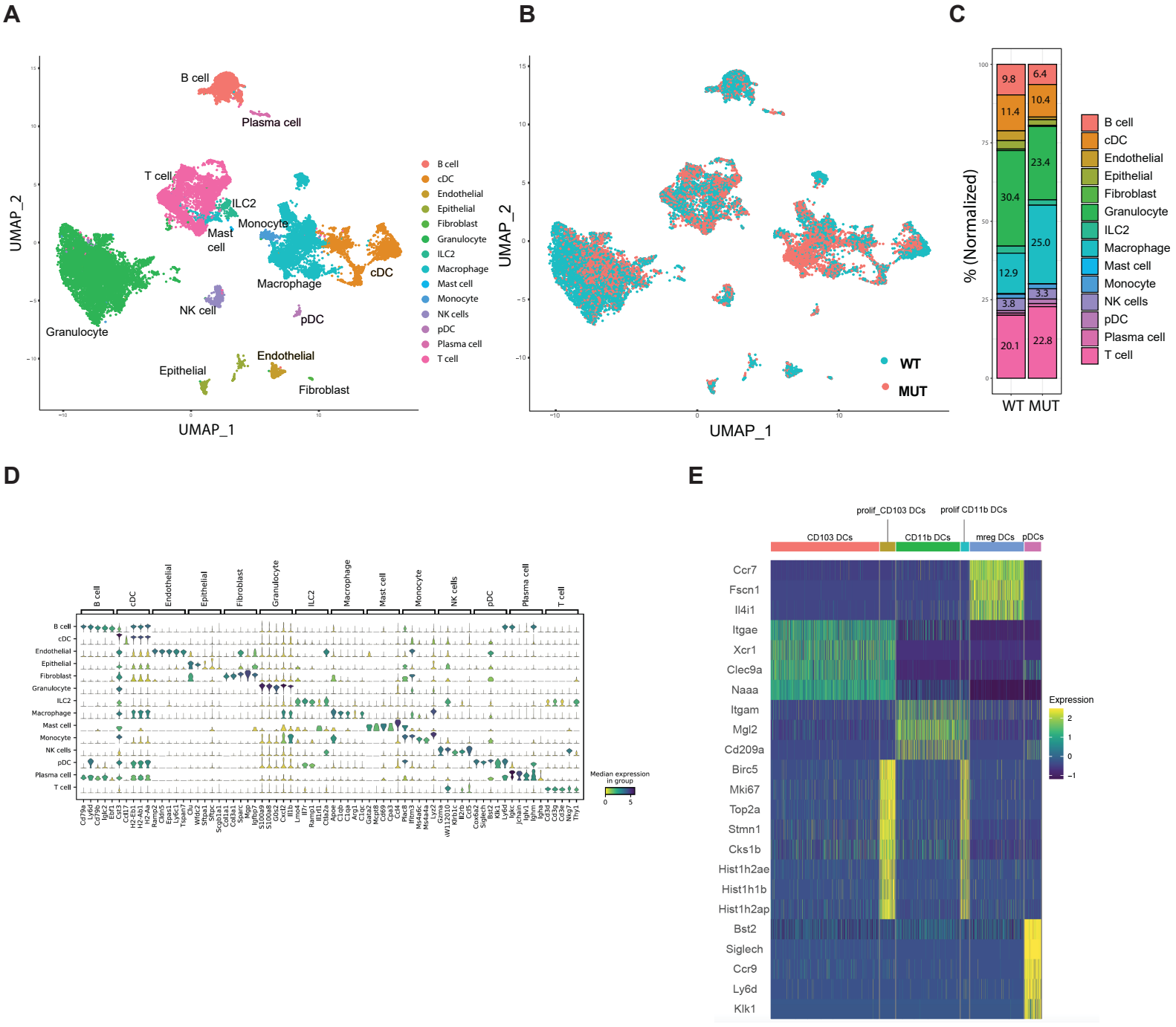
A
B cell
Plasma cell
T cell
ILC2
Monocyte
Mast cell
cDC
Macrophage
NK cell
pDC
Granulocyte
Epithelial
Endothelial
Fibroblast
UMAP_2
UMAP_1
B cell
cDC
Endothelial
Epithelial
Fibroblast
Granulocyte
ILC2
Macrophage
Mast cell
Monocyte
NK cells
pDC
Plasma cell
T cell
B
UMAP_2
UMAP_1
WT
MUT
C
% (Normalized)
9.8
11.4
30.4
12.9
3.8
20.1
6.4
10.4
23.4
25.0
3.3
22.8
WT MUT
B cell
cDC
Endothelial
Epithelial
Fibroblast
Granulocyte
ILC2
Macrophage
Mast cell
Monocyte
NK cells
pDC
Plasma cell
T cell
D
B cell
cDC
Endothelial
Epithelial
Fibroblast
Granulocyte
ILC2
Macrophage
Mast cell
Monocyte
NK cells
pDC
Plasma cell
T cell
Median expression in group
0
5
E
prolif_CD103 DCs
prolif CD11b DCs
CD103 DCs
CD11b DCs
mreg DCs
pDCs
Ccr7
Fscn1
Il4i1
Itgae
Xcr1
Clec9a
Naaa
Itgam
Mgl2
Cd209a
Birc5
Mki67
Top2a
Stmn1
Cks1b
Hist1h2ae
Hist1h1b
Hist1h2ap
Bst2
Siglech
Ccr9
Ly6d
Klk1
Expression
2
1
0
−1

Fig S3

Supplementary Fig 3: scRNA-seq of orthotopic *Keap1* wild-type and mutant tumors.
(A) UMAP visualization of the different immune cell lineages identified by scRNA-seq, clustered and colored by cell type. Clusters identified based on gene expression. (B) UMAP representation of the distribution of immune cell lineages in *Keap1* wild-type (WT, blue) and mutant (MUT, red) lung tumors. (C) Bar plot showing distribution of the immune cell subsets in *Keap1* wild-type and mutant mouse lung tumors. (D) Stacked violin plots depicting the top 5 differentially expressed genes in each cluster shown in A. (E) Heatmap showing unique molecular identified (UMI) counts of selected bona fide genes with key indicating cell type of origin.

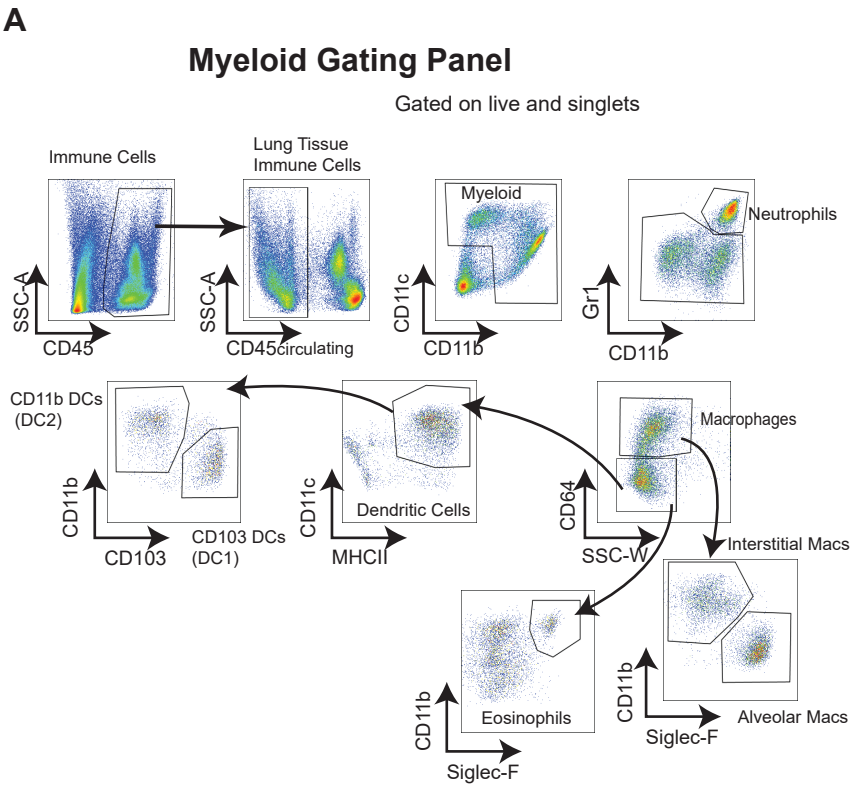
A
Myeloid Gating Panel
Gated on live and singlets
Immune Cells
Lung Tissue Immune Cells
Myeloid
Neutrophils
SSC-A
CD45
SSC-A
CD45circulating
CD11c
CD11b
Gr1
CD11b
CD11b DCs (DC2)
CD11b
CD103
CD103 DCs (DC1)
CD11c
MHCII
Dendritic Cells
Macrophages
CD64
SSC-W
Interstitial Macs
Eosinophils
CD11b
Siglec-F
CD11b
Siglec-F
Alveolar Macs

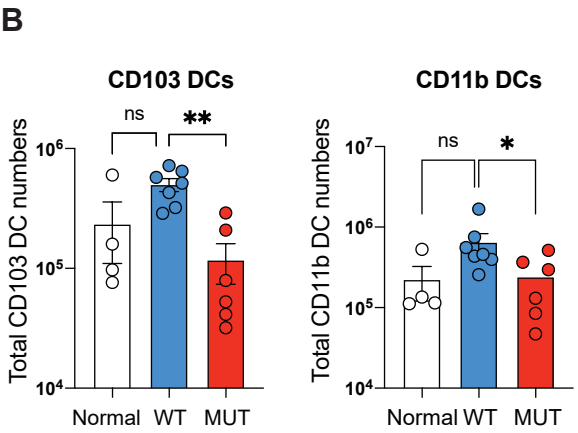
B
CD103 DCs
CD11b DCs
Total CD103 DC numbers
Total CD11b DC numbers
ns
**
ns
*
Normal
WT
MUT
Normal
WT
MUT

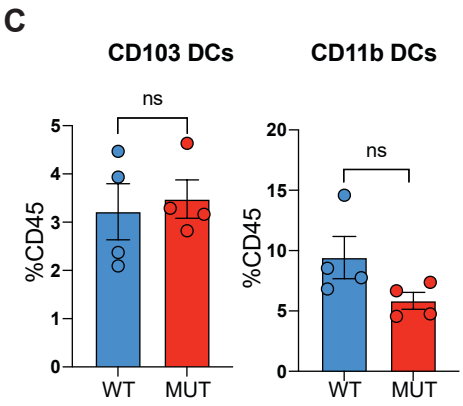
C
CD103 DCs
CD11b DCs
%CD45
%CD45
ns
ns
WT
MUT
WT
MUT

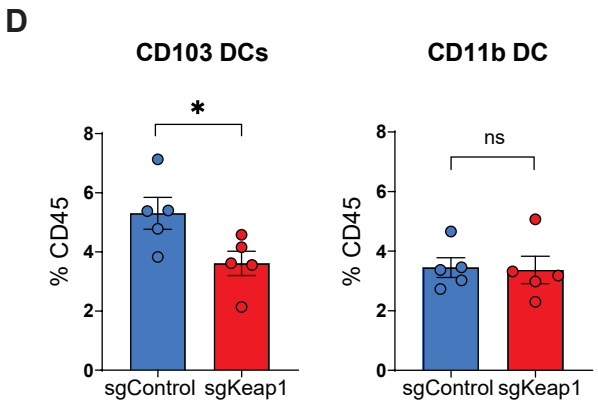
D
CD103 DCs
CD11b DC
% CD45
% CD45
*
ns
sgControl
sgKeap1
sgControl
sgKeap1

Fig. S4

Supplementary Fig 4: **Impact of *Keap1* loss on Dendritic Cells**. (A) Gating strategy for myeloid cell lineage. (B) Total cell numbers of CD103 and CD11b dendritic cells in healthy non-tumor bearing (Normal) lungs and lungs with orthotopic *Keap1* wild-type (WT) and mutant (MUT) tumors. Each symbol represents an individual mouse. (C, D) Analysis of orthotopic tumors showing percentage of CD103 and CD11b DCs out of total tissue-infiltrating immune cells (CD45+CD45circ-) in *Keap1* wild-type and mutant tumors established in male hosts (C) and *Keap1* knockout (sg*Keap1*) and controls established in female hosts (D) . *P<0.05; **P<0.01

A

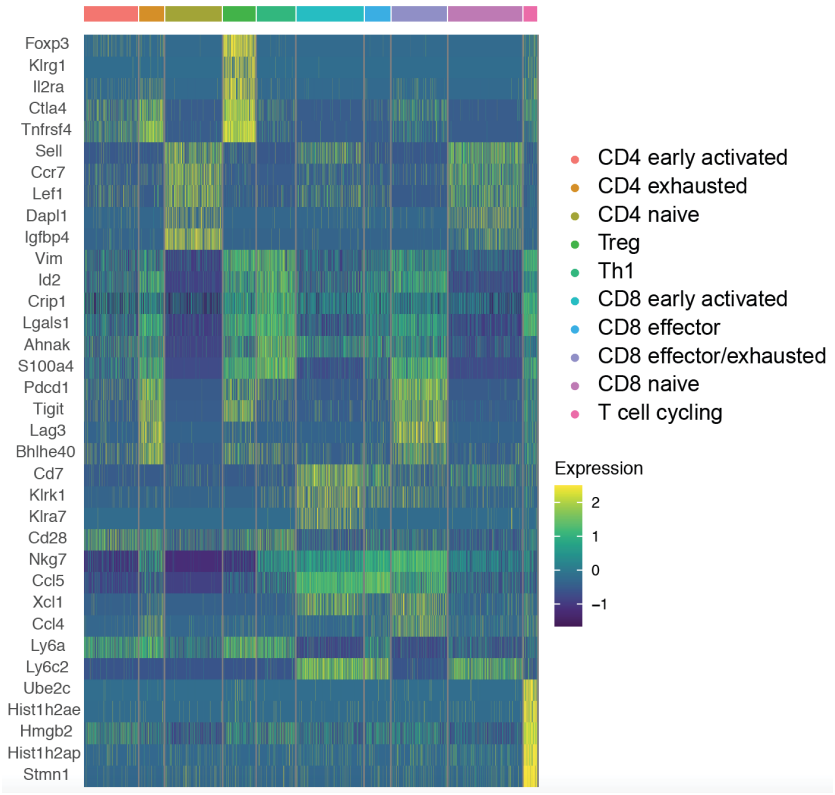
Foxp3
Klrg1
Il2ra
Ctla4
Tnfrsf4
Sell
Ccr7
Lef1
Dapl1
Igfbp4
Vim
Id2
Crip1
Lgals1
Ahnak
S100a4
Pdcd1
Tigit
Lag3
Bhlhe40
Cd7
Klrk1
Klra7
Cd28
Nkg7
Ccl5
Xcl1
Ccl4
Ly6a
Ly6c2
Ube2c
Hist1h2ae
Hmgb2
Hist1h2ap
Stmn1
CD4 early activated
CD4 exhausted
CD4 naive
Treg
Th1
CD8 early activated
CD8 effector
CD8 effector/exhausted
CD8 naive
T cell cycling
Expression
2
1
0
−1

B

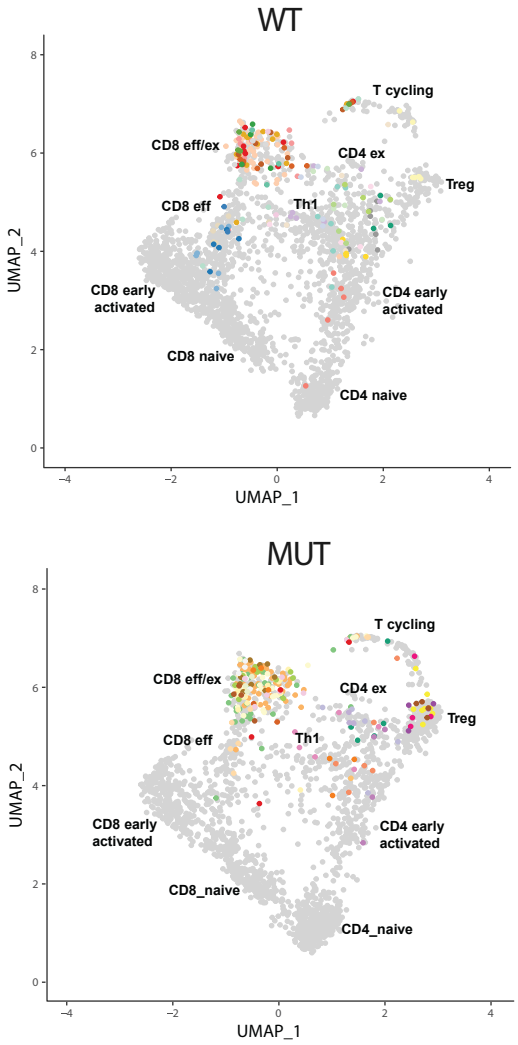
WT
T cycling
CD8 eff/ex
CD4 ex
Treg
CD8 eff
Th1
CD8 early activated
CD4 early activated
CD8 naive
CD4 naive
UMAP_2
UMAP_1
MUT
T cycling
CD8 eff/ex
CD4 ex
Treg
CD8 eff
Th1
CD8 early activated
CD4 early activated
CD8_naive
CD4_naive
UMAP_2
UMAP_1

Fig. S5

Supplementary Fig 5: Single cell analysis identifies T cell subtypes and T cell clonality. (A) Heat map shows normalized and log-transferred unique molecular identified (UMI) counts of selected genes, with key indicating T cell type. (B) UMAP visualization of TCR rearrangement on T cell subclusters of *Keap1* wild-type (WT) and mutant (MUT) tumors. Colored symbols indicate clonally expanded T cells while grey dots indicate polyclonal T cells or T cells that TCR was not reconstructed.

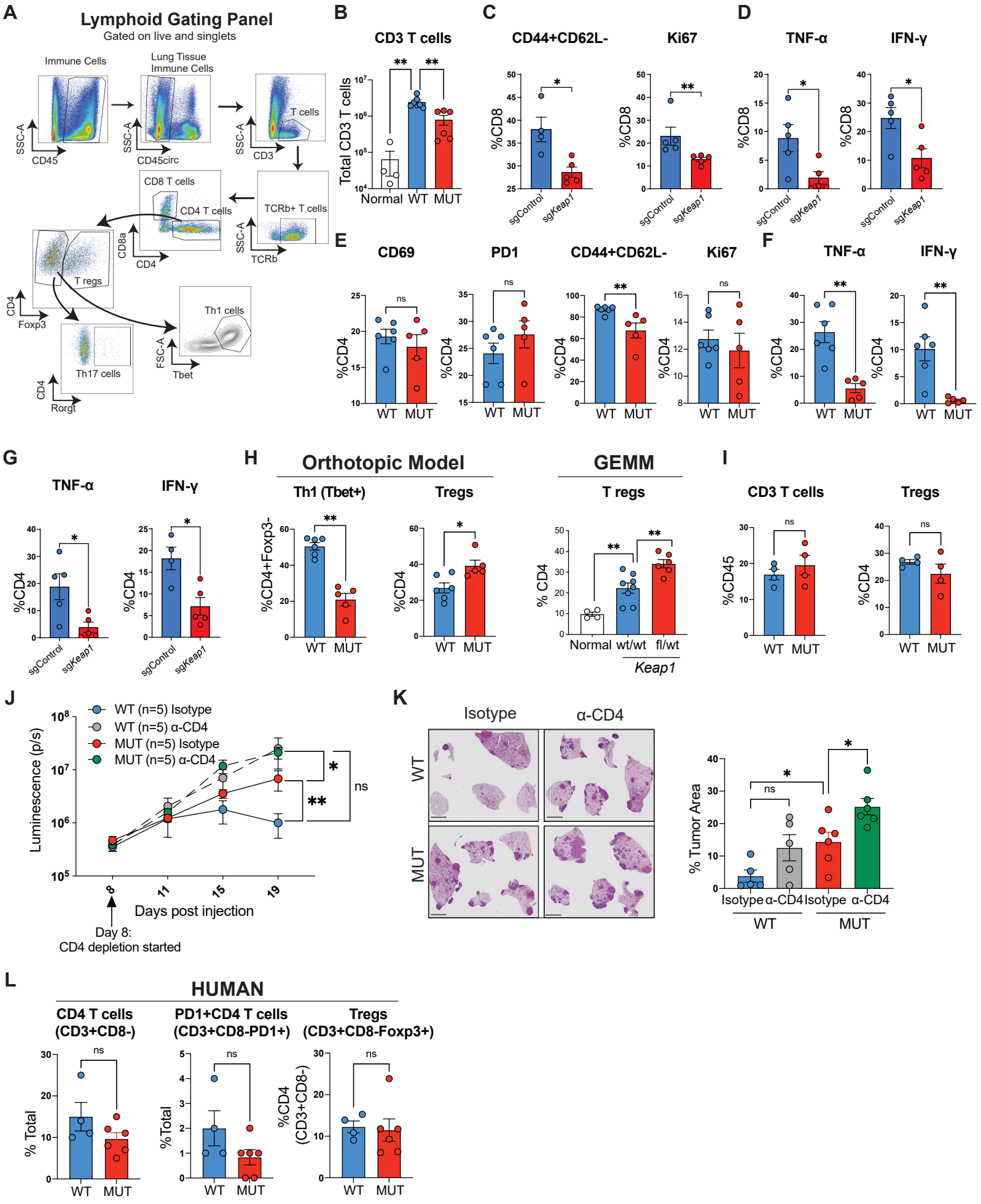
A
Lymphoid Gating Panel
Gated on live and singlets
Immune Cells
Lung Tissue Immune Cells
T cells
CD8 T cells
CD4 T cells
TCRb+ T cells
T regs
Th1 cells
Th17 cells
SSC-A
CD45
CD45circ
CD3
CD8a
CD4
TCRb
Foxp3
FSC-A
Tbet
Rorgt
B
CD3 T cells
Total CD3 T cells
Normal WT MUT
C
CD44+CD62L-
Ki67
%CD8
sgControl
sgKeap1
D
TNF-α
IFN-γ
E
CD69
PD1
CD44+CD62L-
Ki67
%CD4
WT MUT
ns
F
TNF-α
IFN-γ
G
TNF-α
IFN-γ
H
Orthotopic Model
Th1 (Tbet+)
Tregs
%CD4+Foxp3-
GEMM
T regs
% CD4
Normal wt/wt fl/wt
Keap1
I
CD3 T cells
Tregs
%CD45
J
WT (n=5) Isotype
WT (n=5) α-CD4
MUT (n=5) Isotype
MUT (n=5) α-CD4
Luminescence (p/s)
Days post injection
Day 8:
CD4 depletion started
ns
K
Isotype
α-CD4
WT
MUT
% Tumor Area
Isotype α-CD4 Isotype α-CD4
WT
MUT
L
HUMAN
CD4 T cells (CD3+CD8-)
PD1+CD4 T cells (CD3+CD8-PD1+)
Tregs (CD3+CD8-Foxp3+)
% Total
%Total
%CD4 (CD3+CD8-)
WT MUT
ns

Fig. S6

Supplementary Fig 6: *Keap1*-mutant tumors modulation of CD8 and CD4 anti-tumor immune responses

(A) Gating strategy for lymphoid lineage cells. (B) Total cell numbers of CD3 T cells in healthy (non-tumor bearing) lungs and lungs with orthotopic *Keap1* wild-type (WT) and mutant (MUT) tumors. Each symbol represents an individual mouse. (C, D) Percentage of CD44+CD62L- (C), Ki67 (C), TNF-α (D), and IFN-γ (D) expression among CD8 T cells in *Keap1* knockout (sg*Keap1*) tumors compared to controls. Each symbol represents an individual mouse. (E) Percentage of CD69, PD1, CD44+CD62L-, and Ki67 lymphocytes among CD4 T cells in wild-type and mutant *Keap1* tumors. Each symbol represents an individual mouse. Each experimental subgroup had n≥5 mice. (F, G) Percentage of intracellular IFN-γ and TNF-α positive cells among the CD4 T lymphocytes in wild-type and *Keap1*-mutant tumors (F) and *Keap1* knockout (sg*Keap1*) tumors and controls (G). Each symbol represents an individual mouse. (H) Percentage of Th1(Tbet+) cells (out of CD4+Foxp3-) and Tregs (out of CD4 T cells) in wild-type and *Keap1*-mutant tumors or autochthonous genetically engineered mouse model (GEMM) $Keap1^{+/+}$ and $Keap1^{fl/+}$ tumors. Each symbol represents an individual mouse. (I) Percentages of T cells (out of total immune cells) and T regs (out of CD4 T cells) in orthotopic *Keap1* wild-type and mutant tumors established in male hosts. Each symbol represents an individual mouse. (J) Growth kinetics of *Keap1* wild-type and mutant tumors in female hosts upon antibody-mediated CD4 T cell depletion. Depletion was initiated at Day 8 after verifying tumor engraftment and continued until experimental endpoint. Right: Endpoint luminescence for experiment on the left. Each symbol represents an individual mouse. (K) Representative images of lung tumor burden and quantification (tumor area/total lung area) by H&E staining. Scale bars are 2 mm. (L) Quantification of Th cells (CD3+CD8-), PD1+ Th cells (CD3+CD8-PD1+) and Tregs (CD3+CD8-Foxp3+) in *KEAP1* wild-type and mutant human tumors. Tumor area was identified based on H&E staining. *P<0.05; **P<0.01

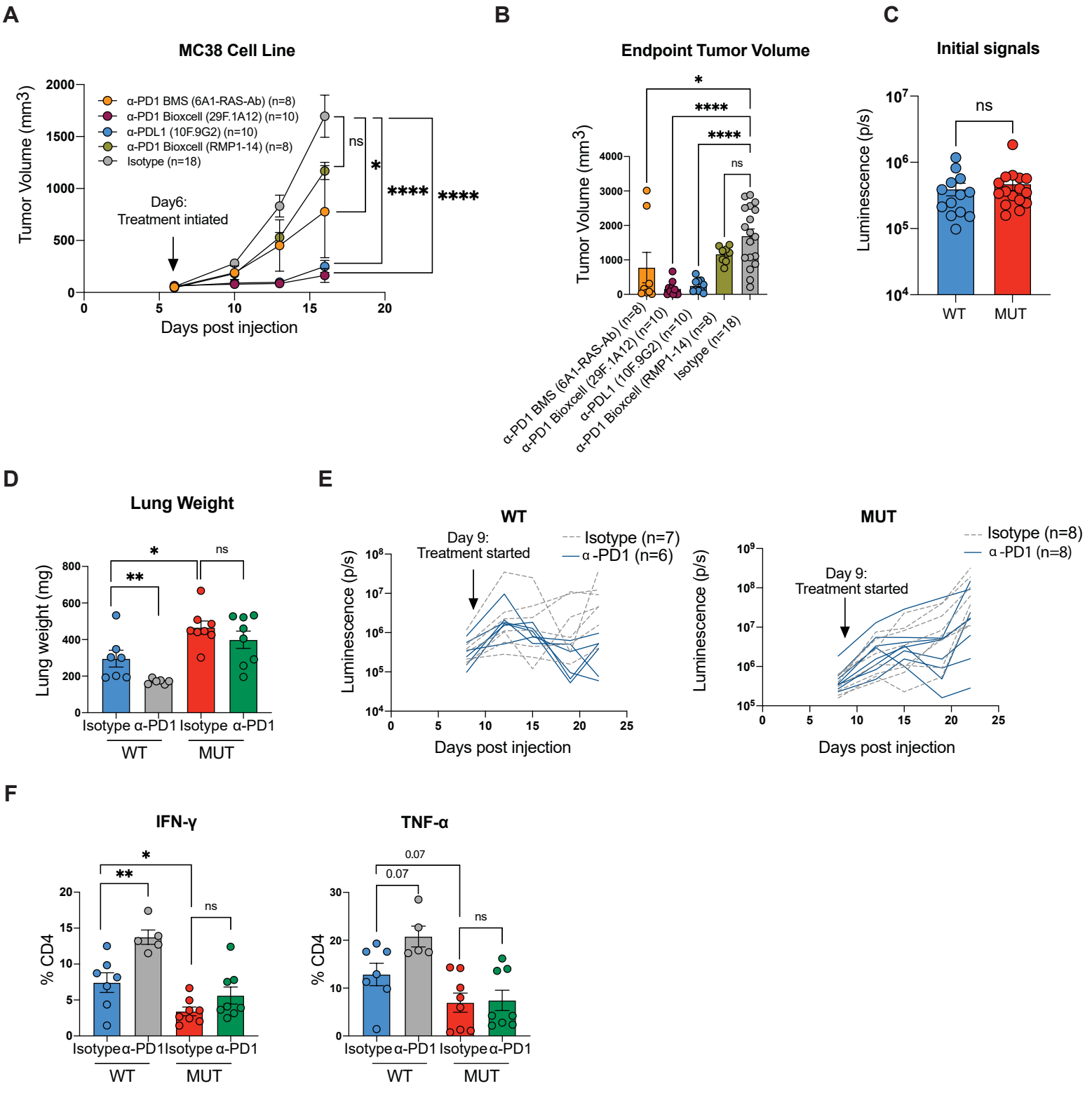
A
MC38 Cell Line
Tumor Volume (mm3)
Days post injection
α-PD1 BMS (6A1-RAS-Ab) (n=8)
α-PD1 Bioxcell (29F.1A12) (n=10)
α-PDL1 (10F.9G2) (n=10)
α-PD1 Bioxcell (RMP1-14) (n=8)
Isotype (n=18)
Day6:
Treatment intiated
ns
*
****
****
B
Endpoint Tumor Volume
Tumor Volume (mm3)
C
Initial signals
Luminescence (p/s)
ns
WT
MUT
D
Lung Weight
Lung weight (mg)
Isotype α-PD1 Isotype α-PD1
WT
MUT
E
WT
Day 9:
Treatment started
Isotype (n=7)
α -PD1 (n=6)
Luminescence (p/s)
Days post injection
MUT
Isotype (n=8)
α -PD1 (n=8)
F
IFN-γ
TNF-α
% CD4
0.07
Isotype α-PD1 Isotype α-PD1
WT
MUT

Fig. S7

Supplementary Fig 7: Immune checkpoint blockade therapy in syngeneic mouse models.

(A) Optimization of immune checkpoint blockade (ICB) antibodies in MC38 colon adenocarcinoma tumors. Tumor growth of MC38 cells subcutaneously injected in the right and left flanks of C57BL/6J mice was measured following treatment with various widely used immune checkpoint inhibitors. Treatment for all antibodies was initiated on Day 6, and continued until experimental endpoint, except for anti-PDL1 which was administered for a total of 3 doses. For isotype control, mice treated with various isotypes were pooled together as no differences were observed between the different isotype control antibody injections. Experimental subgroups treated with an anti-PD1 antibody or anti-PDL1 had $\geq$5 mice. Experimental subgroups treated with isotype control antibody had at least n$\geq$3 mice. (B) Tumor volume at endpoint for the experiment in A. Each symbol represents an individual tumor. (C) Luminescence signals 24hrs prior to a-PD1 treatment initiation of *Keap1* wild-type (WT) and mutant (MUT) KP lung tumors shown in Fig. 4A. Each symbol represents an individual mouse. (D) Lung weight as proxy for tumor burden in mice bearing *Keap1* wild-type and mutant tumors treated with isotype control or anti-PD1. Each experimental subgroup had n$\geq$6 mice. Each symbol represents an individual mouse. (E) ICB responses in individual mice for data shown in Fig. 4A. (F) Percentage of intracellular IFN-γ and TNF-α positive T cells among the CD4 T cells in the wild-type and mutant *Keap1* tumors treated with anti-PD1 or isotype control. Each symbol represents an individual mouse. Each experimental subgroup had n$\geq$5 mice. *P<0.05; **P<0.01; ****P < 0.0001

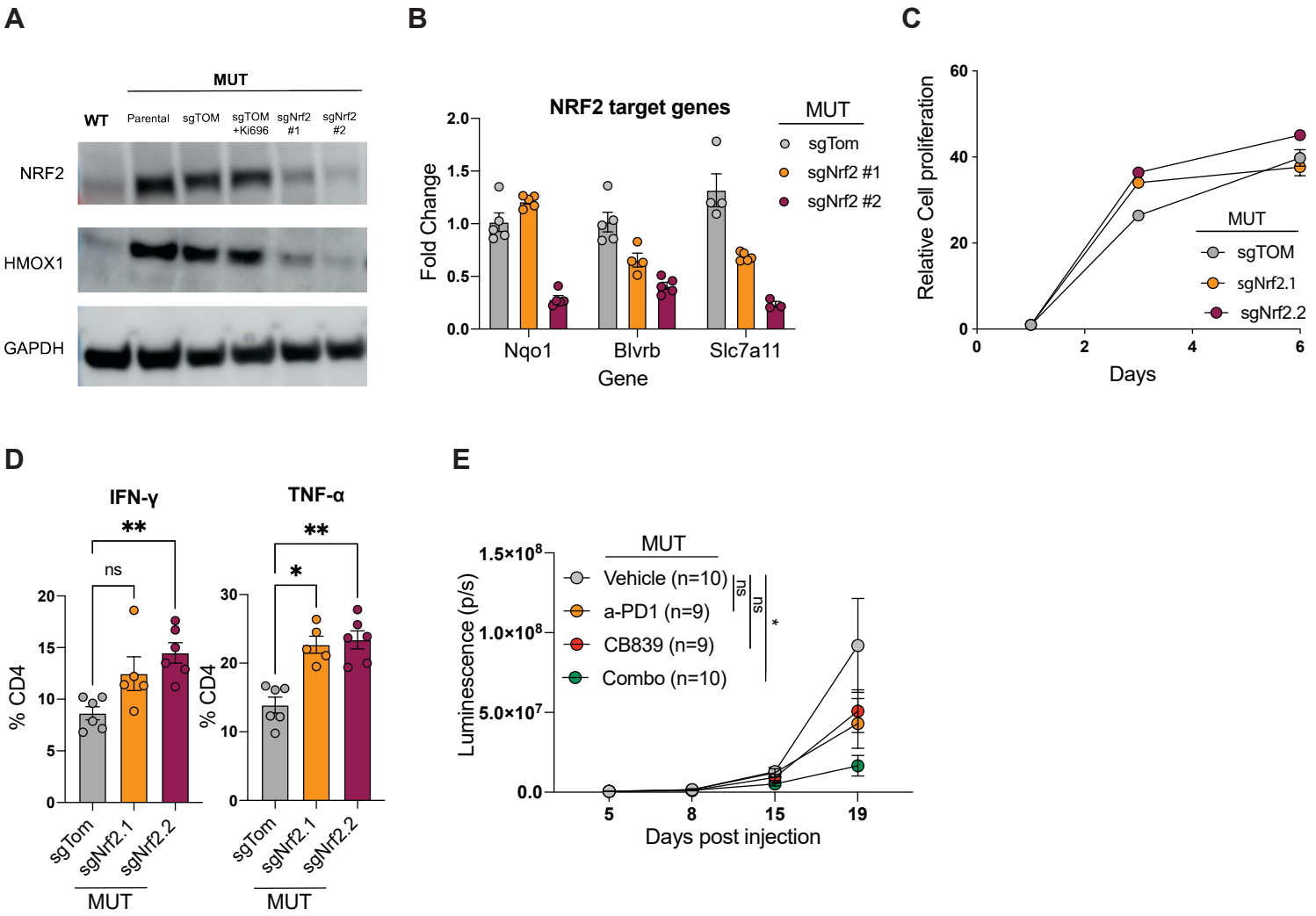
A
MUT
WT
Parental
sgTOM
sgTOM +Ki696
sgNrf2 #1
sgNrf2 #2
NRF2
HMOX1
GAPDH
B
NRF2 target genes
MUT
sgTom
sgNrf2 #1
sgNrf2 #2
Fold Change
Nqo1
Blvrb
Slc7a11
Gene
C
Relative Cell proliferation
MUT
sgTOM
sgNrf2.1
sgNrf2.2
Days
D
IFN-γ
TNF-α
% CD4
ns
sgTom
sgNrf2.1
sgNrf2.2
MUT
E
MUT
Vehicle (n=10)
a-PD1 (n=9)
CB839 (n=9)
Combo (n=10)
Luminescence (p/s)
Days post injection

Fig. S8

Supplementary Fig 8: Validation of *Nrf2*-deficient *Keap1*-mutant cells and synergy of glutamine modulation with ICB in *Keap1*-mutant tumors. (A) Western blot showing NRF2 and HMOX1, an NRF2 target gene, in *Keap1*-mutant (MUT) KP cells transduced with control sgTomato guide or two guides targeting *Nrf2*. Guides targeting *Nrf2* were validated. *Keap1* wild-type KP cell line (WT) was used as a control for low expression of NRF2 and HMOX1 while Ki696 small molecule NRF2 activator was used as positive control. GAPDH was used as a loading control. (B) Gene expression of NRF2 target genes in *Keap1*-mutant KP cells wild-type or deficient for *Nrf2*. (C) *In vitro* proliferation analysis of KP cell lines transduced with control guide against Tomato (sgTom) or against *Nrf2* gene (sgNrf2.1, sgNrf2.2) reveals no difference in growth kinetics. (D) Percentage of intracellular IFN-γ and TNF-α positive cells among the CD4 T lymphocytes. Each symbol represents an individual mouse. Each experimental subgroup had $n \geq 5$ mice. (E) Growth kinetics of *Keap1*-mutant lung orthotopic tumors in C57BL/6J female mice upon treatment of vehicle/isotype control, CB839, α-PD1 or combination of CB-839 and α-PD1. Tumor cells express luciferase enabling monitoring of tumor growth kinetics via luminescence *P<0.05; **P<0.01